CALCULATIONS ON HIGH-ENERGY ELECTRON COOLING IN THE HESR*

D. Reistad, B. Gålnander, K. Rathsman, The Svedberg Laboratory, Uppsala University, Sweden
A. Sidorin, Joint Institute of Nuclear Research, Dubna, Russia

Abstract

PANDA will make use of a hydrogen pellet target. We discuss the choice of beam size at the target and emittance stabilization, and show some results of simulations made with BETACOOL. The simulations include the effects of the internal target, intra-beam scattering, electron cooling and in some cases also stochastic cooling.

HYDROGEN PELLET TARGET

In order to achieve luminosities in PANDA in the range $2\times10^{31} - 2\times10^{32}$ cm^{-2}s^{-1} with $10^{10} - 10^{11}$ stored antiprotons in HESR, an internal hydrogen target with thickness 4×10^{15} cm^{-2} is required. A hydrogen pellet target [1] is the only known kind of internal target, which meets this requirement. At the same time, the granular nature of this target will cause a temporally varying luminosity, particularly if the antiproton beam has small transverse dimensions compared to the vertical separation between pellets or the diameter of the pellet stream.

The hydrogen pellets move in a well-collimated cylindrical flow in which they are distributed rather uniformly, see figure 1. Experience from the use of the pellet target at CELSIUS [2] shows that the pellet flux diameter can be varied between about 1.5 and 3 mm by changing the size of a skimmer in the pellet generator. Since PANDA requires a very big luminosity, we have here chosen to assume that the pellet stream will have a diameter of 3 mm.

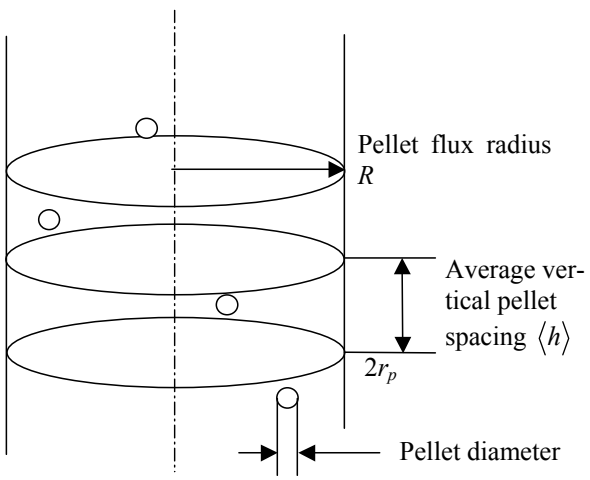

Figure 1: Schematics of the pellet target geometry. The pellets move from top to bottom with the same speed.

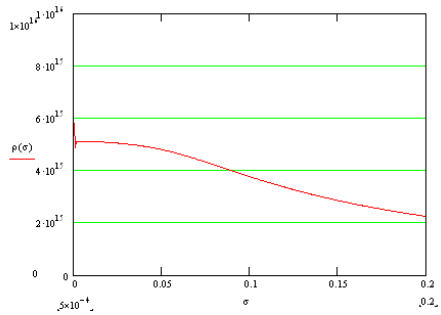

Figure 2: Mean effective target thickness in atoms/cm^3 as a function of the horizontal rms. beam size (in cm). Calculated for Gaussian distribution.

The required target thickness is then met if the average vertical separation between the pellets $\langle h \rangle$ is about 4 mm, which is what we have assumed in the following. With a pellet speed of 60 m/s, this corresponds to a pellet rate of 15,000 s^{-1}, which is well within the achieved performance of the hydrogen pellet target.

CHOICE OF BEAM SIZE AT TARGET

If the horizontal antiproton beam size on the target is made too large, then the luminosity will be reduced due to poor overlap between the beam and the target. The expression for a Gaussian beam is

$$\rho_{\text{eff,mean}} = \frac{\langle \Re \rangle}{\sqrt{2\pi}\sigma_x} \int_{-R}^{R} 2\sqrt{R^2 - x^2}\, \exp\left(-\frac{x^2}{2\sigma_x^2}\right) dx$$

where

$$\langle \Re \rangle = \frac{\frac{4}{3}\pi r_p^3}{\pi R^2 \langle h \rangle} \Re; \quad \Re = 4.3\times10^{22} \text{ atoms/cm}^3$$

This effect is illustrated for our parameters in figure 2. We see that the horizontal r.m.s. beam size should not be chosen bigger than about 0.8 mm in order to keep the effective luminosity above 80 % of the maximum possible.

At the same time, if the beam size is chosen too small, then the granular nature of the pellet target will cause fluctuations in the effective target thickness. For a Gaussian beam, the maximum instantaneous effective target thickness, which occurs when the beam hits a pellet head-on, is given by

* Work supported by Uppsala University and by EU Design Study Contract 515873, DIRACSecondary-Beams

$$\rho_{\text{eff,max}} = \frac{\Re}{2\pi\sigma_x\sigma_y}\int_{-r_p}^{r_p}\int_{-\sqrt{r_p^2-x^2}}^{\sqrt{r_p^2-x^2}} 2\sqrt{r_p^2-x^2-y^2}\times$$

$$\times\exp\left(-\frac{x^2}{2\sigma_x^2}-\frac{y^2}{2\sigma_y^2}\right)dydx$$

The ratio between the maximum and average luminosity is plotted as the ratio between $\rho_{\text{eff,max}}$ and $\rho_{\text{eff,mean}}$ according to these formulae, and also according to the approximate formula given in [3], is shown in figure 3.

In fact, the beam distribution is not going to be Gaussian, but more like a square with rather homogeneous density of antiprotons up to a certain dimension, see figure 10 below. In the following, we define our transverse beam size as the beam size, which contains 50 % of the particles.

We choose a "square" beam spot with side $2\times 0.8 = 1.6\,\text{mm}$ in both planes, which gives a ratio between maximum and mean luminosity of about 3 and about 80 % of the maximum possible average luminosity, which we believe is an acceptable compromise.

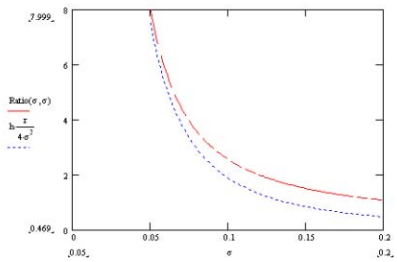

Figure 3: Ratio between maximum and mean effective luminosity as a function of rms beam size (in cm), assumed to be the same in both planes. The lower curve is according to the simplified formula in [3].

CHOICE OF BETA VALUE AT TARGET

Conventional wisdom tells that the beta value at the target should be chosen as small as possible, in order to get the best single-scattering lifetime of the beam. We have

$$\sigma_{\text{single scattering}} = \pi\left(\frac{2r_e m_e c^2}{cp\beta}\right)^2\cdot\frac{\beta_T}{A}$$

where A is the acceptance of the ring. However, choosing very small β_T will make the maximum beta value in the neighbouring quadrupoles large, which may make the acceptance small, see figure 4. In HESR, the diameter of the quadrupole vacuum chambers is planned to be 89 mm, and PANDA requires the diameter of the vacuum chamber at the pellet target to be 20 mm. Therefore, we can assume that the horizontal and vertical acceptances are given by:

$$A_{x,y} = \min\left(\frac{(44.5\,\text{mm})^2}{\beta_{x,y,\max}}, \frac{(10\,\text{mm})^2}{\beta_{x,y,T}}\right)$$

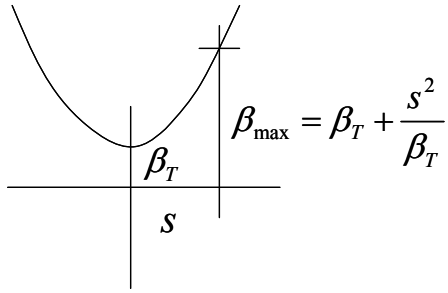

Figure 4: Choosing the beta value at the target too small does not significantly improve single-scattering lifetime, because the beta value in the neighbouring quadrupoles becomes correspondingly larger.

Inspecting a MAD file for HESR [4] indicates the following approximate relationships between $\beta_{\max}$ and β_T:

$$\beta_{x,\max} = \beta_{x,T} + \frac{300\,\text{m}^2}{\beta_{x,T}};\ \beta_{y,\max} = \beta_{y,T} + \frac{550\,\text{m}^2}{\beta_{y,T}}$$

Inspecting these formulae shows that if the beta values at the target are chosen below 4 m, then they have almost no effect on the single scattering cross section. On the other hand, if the beta values are chosen above 4 m, then the single-scattering cross section will grow as β_T^2. We choose $\beta_{x,T} = \beta_{y,T} = 4\,\text{m}$ for 1.5 GeV/c, but 8 m for intermediate energies and 16 m for 15 GeV/c. The single-scattering cross section remains much smaller than the nuclear cross section for all momenta from 3.8 GeV/c and up.

TRANSVERSE EMITTANCE

The choice of $\beta_{x,T} = \beta_{y,T} = 8\,\text{m}$ at intermediate energies together with the chosen beam spot on the target of 0.8 mm implies that the transverse emittance should be 8×10^{-8} m. For the lowest and highest energies required transverse emittances are 1.6×10^{-7} m and 4×10^{-8} m respectively.

ELECTRON BEAM

The task of the electron cooling system is to reduce the energy spread of the antiproton beam to a few 10^{-5}. This corresponds to a longitudinal temperature of the antiprotons of about 0.1 eV, and can only be achieved with magnetized electron cooling. The magnetic flux in the electron beam is limited for technical reasons to $0.07\times\pi\times0.0085^2\,\text{Tm}$ [5]. We have chosen an electron beam diameter on the cooling section of 10 mm and a magnetic field of 0.2 T. For a transverse electron temperature of 1 eV this magnetic field strength gives a cyclotron radius of 1.7×10^{-5} m and at 8 GeV a typical distance between electrons $n_e^{-1/3}$ of 7.7×10^{-4} m, which means that magnetized electron cooling can take place. The reason for the choice of electron beam diameter is that we wish the antiproton beam to remain essentially inside of the electron beam in order to avoid any effects of non-linear

electrical fields outside of the electron beam, which in our opinion still remain to be fully understood [6,7]. We have therefore also chosen the beta value in the electron cooler to be only $10 \times \beta_T$, i.e. 80 m at intermediate energies. Then, the "square" antiproton beam will have a side of half of the electron beam diameter, and thus the antiprotons will essentially go inside of the electron beam.

SUMMARY OF PARAMETERS USED IN COMPUTATIONS

The following parameters have been used in the computations reported here:

effective length of electron cooler	20 m
electron current	1 A (0.2 A @ 1.5 GeV/*c*
electron beam radius, uniform cylinder	5 mm
magnetic field in electron cooler	0.2 T
beta value at electron cooler (both H and V)	80 m (40, 160 m @ 1.5, 15 GeV/*c*)
transverse electron temperature (in centre of electron beam)	1 eV
Transverse gradient of electron velocity (in order to take unavoidable envelope oscillations into account. The chosen value corresponds to a cyclotron radius at the edge of the electron beam of 0.1 mm, or 35 eV)	7×10^8 s^{-1}
longitudinal electron temperature	0.5 meV
electron beam neutralization	nil
cooling force model	Parkhomchuk
rms. straightness of magnetic field lines	1×10^5 radians
hydrogen pellet target, pellet size	30 μm
pellet stream diameter	3 mm
vertical separation between pellets	4 mm
beta value (both planes) at target	8 m (4, 16 m @ 1.5, 15 GeV/*c*)
nuclear reaction cross section	100, 70, 55, 50 mbarn @ 1.5, 3.8, 8.9, 15 GeV/*c*.
intra-beam scattering	Martini model
barrier bucket voltage	200 V
barrier duration (relative to circumference)	10 %

EMITTANCE STABILIZATION

If special precautions were not to be taken, then the electron cooling would reduce the transverse emittance below the wanted value. This would make the antiproton beam size on the target too small and also the momentum spread increase due to intra-beam scattering.

Three different methods for stabilization of the emittance have been discussed:

- use of a "hollow" electron beam [8]
- application of white noise in the transverse degrees of freedom
- intentional misalignment ("tilt") of the electron beam with respect to the antiproton beam.

The "hollow" electron beam will be efficient for ion beam storage using cooling-stacking procedure. The low electron density in the stack region avoids overcooling of the stack and decreases (for heavy ions) recombination in the cooling section. In the HESR, where very small momentum spread is wanted, the hollow beam will not be suitable, because cooled antiprotons will only see a small

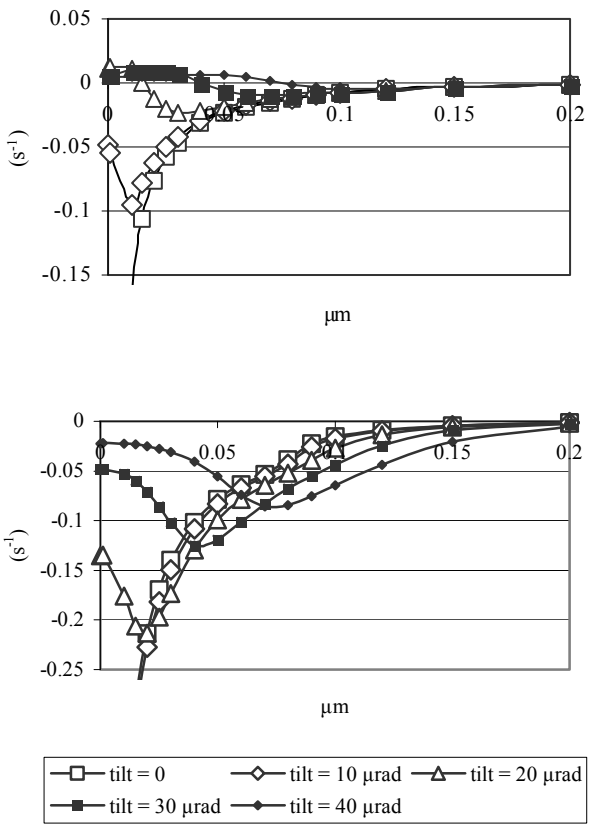

Figures 4 – 5: Transverse and longitudinal cooler rates at 8 GeV for different tilts.

electron density and the longitudinal cooling force will therefore be correspondingly smaller.

Another unknown with the hollow electron beam will be due to the non-linear electrical fields, that the antiprotons will be seeing. These fields may be particularly damaging in the case of hollow beam [9].

Transverse heating by additional noise has been tried at a few rings to suppress coherent instabilities. However, the experience has been, that the transverse heating decreases the beam lifetime, and leads to increase not only of emittance, but also of momentum spread.

Many experiments have shown, that a controlled misalignment is a powerful tool to control the transverse emittance of a stored beam. When the tilt reaches a cer-

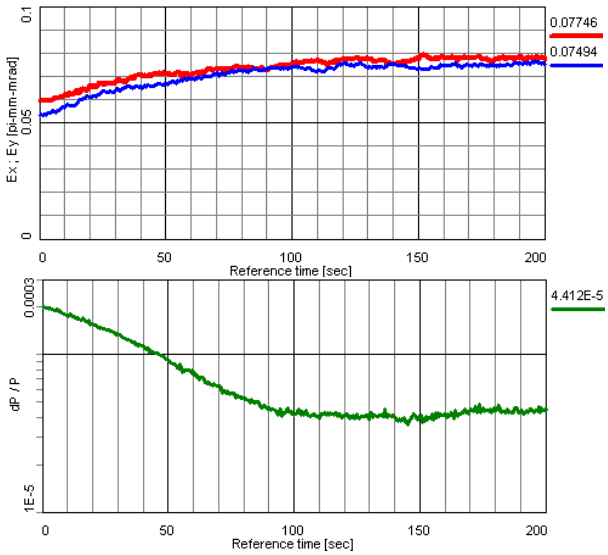

Figures 6–7: The calculated evolution of the beam under the influence of the hydrogen pellet target, electron cooling and intra-beam scattering of horizontal and vertical emittances and momentum spread of a beam of 10^{10} antiprotons of 8.9 GeV/c.

tain threshold the particles start to oscillate with a certain value of betatron amplitude [10]. This amplitude depends on the tilt angle, and the beam emittance cannot be less than the value corresponding to the oscillation amplitude. In absence of other effects, the beam profile has a specific double-peak structure.

These oscillations are caused by the non-linearity of the friction force. The force has a maximum at a certain relative velocity, and the oscillations begin when the transverse velocity of the misaligned electron beam is equal to the velocity, which is corresponding to the maximum of the force. This transition from stable particle motion, described by a fix-point attractor in the centre of phase space, to oscillating motion corresponding to a circular attractor is known as a "Hopf bifurcation".

In the absence of the internal target, the beam distributions become significantly denser near the circular attractor. The density does become smeared by the target and typically gets rather flat. However, if the dip in the middle of the distribution would become too important, then a solution can be to turn off the intentional tilt during short

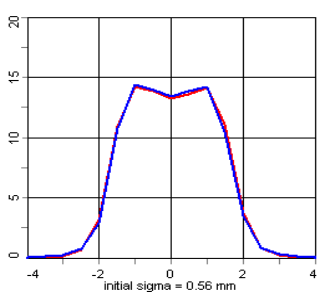

Figure 8: Calculated equilibrium transverse beam profiles of 10^{10} 8 GeV electron-cooled antiprotons on target in units of the initial rms. beam size of 0.56 mm.

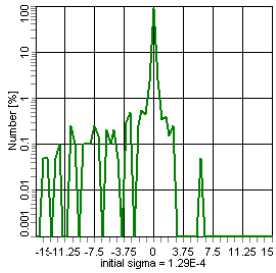

Figure 9: Calculated equilibrium momentum distribution of 10^{10} 8 GeV electron-cooled antiprotons on target in units of the initial rms. momentum spread of 1.29×10^{-4}.

intervals. This will re-create the attractor in the middle of the distribution.

The emittance stabilization by tilting the electron beam with respect to the antiproton beam illustrated in figures 4 – 5, where the growth rates due to electron cooling are shown as a function of transverse Courant-Snyder invariant for different tilts. The calculation is made in BETACOOL [11] using the Parkhomchuk cooling model [8]. The rates can be compared to the heating rates caused by the hydrogen pellet target, which for this energy are approximately $5\times10^{-10}\ \mathrm{m}/\varepsilon\ \mathrm{s}^{-1}$ in the transverse planes (where ε is the Courant-Snyder invariant), and $3\times10^{-10}\Big/\left(\frac{\Delta p}{p}\right)^2\ \mathrm{s}^{-1}$ in the longitudinal plane. This indicates that at $\varepsilon = 0.08$ μm the equilibrium $\Delta p/p$ between target heating and electron cooling would be about 7×10^{-5}. In the tracking computation, we arrive at 4.4×10^{-5} for 90 % of the antiprotons.

RESULTS

Calculations were made with BETACOOL [11]. They were carried out for a beam of 10^{10} antiprotons (except when stated otherwise) at 1.5, 3.8, 8.9, and 15 GeV/*c*. All calculations were made assuming that the hydrogen pellet target was continuously turned on. At 1.5 GeV/*c* we reduced the electron current to avoid instabilities. We found the tilt angles as stated in the table below. At 15 GeV/*c*, the situation dramatically improved when we included longitudinal stochastic cooling as well as electron cooling in the simulation, see below:

momentum GeV/c	β_T (m)	β_C (m)	tilt (radians)	I_e (A)	$\Delta p/p$ (90 %)
1.5	4	40	6×10^{-5}	0.2	1.3×10^{-5}
3.8	8	80	3.5×10^{-5}	1	9.3×10^{-6}
8.9	8	80	3.5×10^{-5}	1	4.4×10^{-5}
15	16	160	8×10^{-6}	1	1.9×10^{-4}

In agreement with others in the project [12] we have defined the momentum spread as the spread, which contains 90 % of the antiprotons. The transverse emittances

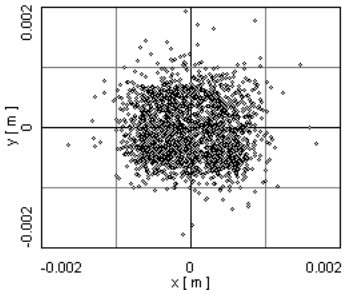

Figure 10: Calculated aspect of the beam on the target for 10^{10} 8 GeV electron-cooled antiprotons on target.

are defined as the areas of the ellipses in phase space, which contain 50 % of the particles, divided by π.

The calculated evolution of horizontal and vertical emittances and momentum spread of a beam of 10^{10} antiprotons of 8.9 GeV/*c* are shown in figures 6 – 7, the calculated equilibrium transverse beam profiles and momentum distribution are shown in figures 8 – 9, and the calculated aspect of the beam on the target in figure 10.

The beam lifetime was ranging from about 3,000 s at 1.5 GeV/*c* to about 7,000 s at 15 GeV/*c*, considering nuclear cross sections and transverse acceptances as discussed above and momentum acceptance 2×10^{-3} [13].

We repeated the calculation at 8.9 GeV/*c* also for 10^{11} antiprotons, see figures 11 – 12. We note that the equilibrium 90 % momentum spread increased from 4.4×10^{-5} to 6.6×10^{-5}.

We note that at high energies the momentum distribution (figure 9) develops a pronounced low-energy tail. We therefore have made another simulation, where we have included longitudinal stochastic cooling as well as electron cooling. For the longitudinal stochastic cooling we used a bandwidth from 2 to 4 GHz [14]. The resulting longitudinal evolution and equilibrium distribution are

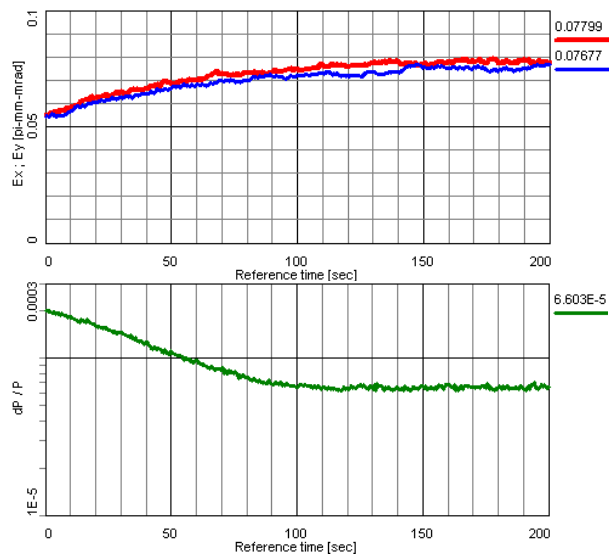

Figures 11 – 12: The calculated evolution of the beam under the influence of the hydrogen pellet target, electron cooling and intra-beam scattering of horizontal and vertical emittances and momentum spread of a beam of 10^{11} antiprotons of 8.9 GeV/c.

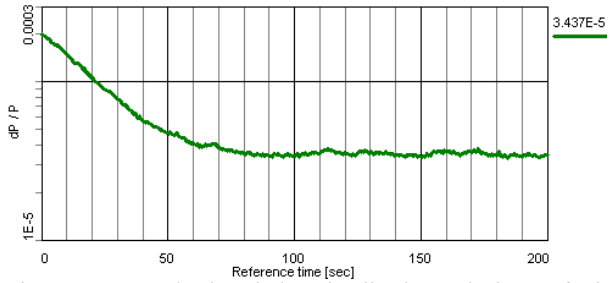

Figure 13: Calculated longitudinal evolution of the beam under the same conditions as in figure 7, but with stochastic cooling as well as electron cooling assumed.

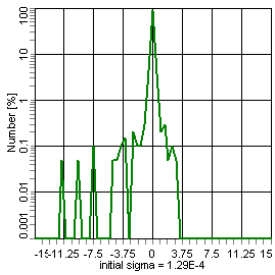

Figure 14: As figure 9 but with stochastic cooling as well as longitudinal cooling.

shown in figures 13-14. The equilibrium 90 % momentum spread went down from 4.4×10^{-5} to 3.4×10^{-5}

We also made a calculation at 15 GeV/*c* where we again included longitudinal stochastic cooling with bandwidth from 2 to 4 GHz as well as electron cooling. The equilibrium momentum spread improved dramatically: from 1.9×10^{-4} to 3.4×10^{-5}.

CONCLUSIONS

We have chosen a "square" beam spot with side 1.6 mm on the pellet target, and shown that by appropriate choice of beta value at the target and suitably tilting the electron beam, this can be combined with achieving very small momentum spread. At high energies, a combination of electron cooling and longitudinal stochastic cooling gives the best performance.

REFERENCES

[1] C. Ekström et al., NIMA 371 (1996) 572.
[2] G. Norman, private communication.
[3] V. Ziemann, NIMA 556 (2006) 641.
[4] Y. Senichev, private communication.
[5] T. Bergmark et al., EPAC2006.
[6] D. Reistad et al., CERN94-03, 183.
[7] J. Dietrich et al., COOL05, 270.
[8] V.V. Parkhomchuk, COOL05, 249.
[9] V. Ziemann, NIMA 556 (2006) 45.
[10] H. Danared et al., EPAC2000.
[11] A. Sidorin, these proceedings.
[12] A. Lehrach, private communication.
[13] R. Maier, private communication.
[14] H. Stockhorst, private communication.